PROCEEDINGS OF SCIENCE

Patch Effect in Drag Free Satellites

V. Ferroni*, D. Hipkins †, A.S. Silbergleit ‡
Gravity Probe B, W.W. Hansen Experimental Physics Laboratory,
Stanford University, Stanford, CA 94305-4085, USA.

To compensate for the non–gravitational orbital disturbances drag free satellites monitor and control their position with respect to a reference body enclosed inside their structure. The body, shielded from the environment, follows a free fall trajectory when its motion can be ideally considered decoupled from that of the spacecraft. Lessons learned from Gravity Probe B and the design of the Satellite Test of the Equivalence Principle experiment strongly motivate the study of the force and torque between the reference body and the spacecraft due to uneven distributions of electrostatic potentials. Additional interest to that comes also from prospective space experiments as Microscope and the Laser Interferometer Space Antenna.

25th Texas Symposium on Relativistic Astrophysics
December 6-10, 2010
Heidelberg, Germany

*Current Address: ferroni@science.unitn.it.; Facolta' di Scienze, Universita' di Trento, Povo, Italia.
†david.hipkins@mavericks7.com; Mavericks7, LLC. Palo Alto, California USA.
‡gleit@stanford.edu

© Copyright owned by the author(s) under the terms of the Creative Commons Attribution-NonCommercial-ShareAlike Licence.

PoS(Texas 2010)253

1. Introduction

Drag free satellites [1, 2] are one of the most stable platforms available nowadays to perform experiments in space. High precision missions like Gravity Probe B (GP–B) and Gravity field and steady-state Ocean Circulation Explorer (GOCE) in the past, and future projects as Microscope, the Satellite Test of the Equivalence Principle (STEP), Laser Interferometer Space Antenna (LISA) and LISA Pathfinder have selected such technology. Its basic principle is that a spacecraft compensates for the non–gravitational orbital disturbances by "flying around" a reference body (TM=Test Mass) enclosed in the inside and thus shielded from the environment. Having the TM virtually subjected to the gravitational field only, the satellite is able to follow a free fall trajectory. Any coupling, unless properly modeled and compensated, leads to deviations of the spacecraft orbit from the nominal free fall path. The electrostatic interactions, among others, turn out particularly important when the gap between the TM and its housing is small as testified by the evidence found during the GP–B mission described below. In fact, the patch effect (PE), i.e., the uneven electrostatic potential pattern on metal surfaces[1], generally causes the force and torque between the satellite and TM; closer the surfaces, the bigger the force and torque are [8, 9].

2. GP–B: Lessons Learned

Launched in 2004 to test General Relativity, GP–B flew four gyroscopes on a drag free satellite in a 642 Km circular polar orbit around the earth [10, 11]. The goal was to measure the precessions of the gyro's angular moment with respect to a reference star due to the frame dragging and geodetic effects. Averaged over the orbital motion of the satellite, both of these predicted effects produce a linear drift in the orientation of the gyroscope spin axis with time, as illustrated in the diagram shown in fig. 1 (see [12]).

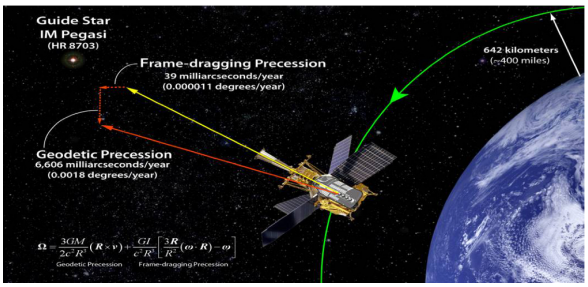

Figure 1: The geodetic and frame–dragging effect as seen on the GP–B orbit.

Since its early days [13], the mission was designed to fly drag free, with one of the science gyroscopes providing the reference of the geodesic for the satellite. Particular care was taken to estimate the interactions between the gyro and spacecraft and minimize them below some required value. Among many other perturbations, PE disturbance was thoroughly studied. Special manufacturing processes for the coating of the gyro and the housing were used to minimize the patch voltages. Despite all this, the PE contribution turned out to be much larger than expected. The

[1] For the origin and some measurements of electric voltages on the surfaces of metals see the pioneering works [3, 4], and then [5]–[7].

PoS(Texas 2010)253

impact of the resulting additional electrostatic force and torque on the system strongly endangered the mission success.

The GP–B science phase started after four months of initial operations needed to properly set up the experiment in space. The data collection continued for nearly twelve months and ended with 46 days period of post–flight calibration, which helped to cope with systematic errors. During this phase it was understood that the gyroscope–housing system had had quite an anomalous behavior. The rotor and housing had developed significant classical torques which superimposed the linear relativistic drift. A thorough analysis led to the discovery of two forms of these torques [9]: the first,

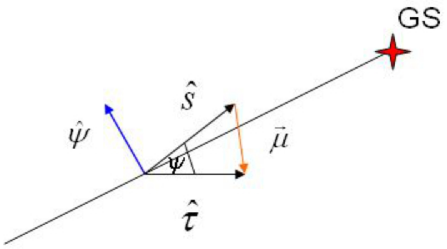

Figure 2: Unit vectors of spin axis, $\vec{s}$, roll axis, $\vec{\tau}$; $\vec{\mu}$ misalignment vector, $\vec{\mu} = \vec{\tau} - \vec{s}; \psi = |\vec{\mu}| \equiv \mu$, to lowest order.

a misalignment torque, had a magnitude proportional to the misalignment angle, ψ when smaller than $\sim 1\,deg$, and generated a drift perpendicular to the misalignment, μ, a small ($\mu < 10^{-4}$) vector connecting the unit vectors along the gyro spin and spacecraft roll axes (see fig.2). The second, a resonance torque, was discovered by studying the obtained gyro orientation hystories. From time to time, the spin direction of one of the gyroscopes would shift by an angle of $20 - 100\,marc - sec$ in just a few days, with no such effect in the other three. These shifts occurred when a high multiple of the slowly changing gyroscope polhode frequency coincided with satellite roll frequency (a roll-polhode resonance).

The source of these torques was found to be the patch potential distributions on the surfaces of the rotor and housing. Expressions for the PE torques were accurately derived, allowing the data analysis team to reconstruct the dynamics of the gyro motion thus providing accurate separation from the relativistic drift [10].

The GP–B experience certainly taught the lesson that analytical modeling of the electrostatic force and torque is fundamental when a experimental set-up includes conducting surfaces in a close proximity to each other, as it happens with the mentioned Microscope, LISA and, in particular, with STEP missions. In the next section we describe STEP set–up in some detail and present the results from our PE study.

3. The STEP Case

STEP, a medium size scientific satellite ($< 900\,Kg$), will be put into a drag free earth orbit at the altitude of $\sim 550\,Km$, [14, 15]. It is to measure the relative free fall acceleration of pairs of TMs of different materials with an accuracy of $10^{-17} m/sec^2$, to determine the equivalence of the

PoS(Texas 2010)253

inertial and gravitational mass with an uncertainty 6 orders of magnitude smaller than the existing results [16], or find violations of the Equivalence Principle (EP; in other words, Universal Free Fall) somewhere between 1 part in 10^{12} and 1 part in 10^{18}.

STEP will fly four differential accelerometers (DAC), each with a pair of TMs shaped as coaxial cylindrical shells. The cross–section of the DAC is shown in fig. 3. An electromagnetic system of magnetic bearings and capacitors keeps TMs alligned and centred to within $< 1nm$. The transverse degrees of freedom are constrained, the two axial ones are left free. A Superconducting Quantum Interference Device similar to that used for the GP–B mission will be used to measure the axial position of the TMs. Its readout will provide the needed data to guide the satellite and to carry out the science measurements. The *common* axial motion of each pair of TMs (namely the

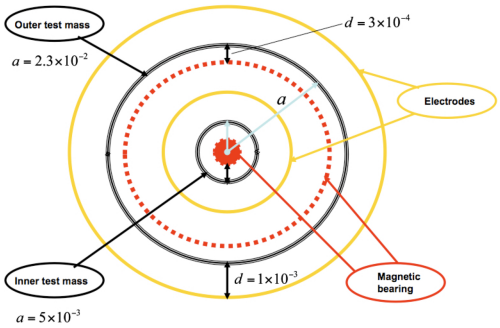

Figure 3: Cross section of the STEP differential accelerometer (all dimensions in meters.)

mean value of the axial displacement of the two TMs forming the DAC) carries the information about non–gravitational disturbances acting on the spacecraft. By compensating for them with the drag free controller, STEP follows a free fall trajectory around the earth. That happens when the interactions between the TM and satellite are negligible as compared to the contributions from the orbital environment. With electromagnetic constraints chosen to meet this requirement, the only potentially dangerous interaction to investigate is the PE, so far. The main question here is whether the electrostatic force due to patches is large enough to dominate the motion of the TM. That would lead to the TM running after the satellite and severely corrupt the spacecraft's drag free control performance.

The test of the Equivalence Principle is performed with the data of the *differential* axial motion of each pair of TMs. Nominally the DACs are kept inertially fixed and the EP violation signal will be at the orbital frequency, $f_{orb} = 1.74 \times 10^{-4} Hz$. However, changing the signal frequency from one measurement session to the other helps to discover and remove systematic readout errors. To achieve this, modulation of the frequency is planned by rolling the satellite (and the DACs) about the normal to the orbital plane at some frequency $f_{roll} \geq 2 f_{orb}$ (the DAC axes lie in the orbital plane as prompted by fig.4). With this procedure, the science signal will be at the frequency $f_s = f_{roll} \pm f_{orb}$ bounded from below as

$$f_s \geq 1.74 \times 10^{-4} Hz\,.$$

However, despite the time signature, the violation signal might still be mimicked if the PE force has

PoS(Texas 2010)253

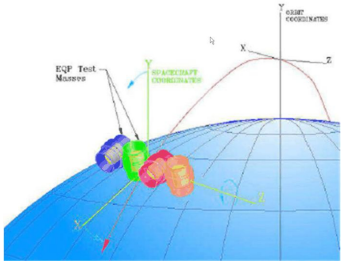

Figure 4: TM set–up in the STEP mission.

a harmonic component in the bandwidth of the science measurement. Moreover, the spin motion of the TM may be responsible for generating interfering harmonics as well.

4. Patch Effect in Cylindrical Geometry

To address these issues in the STEP mission, we studied the electrostatic interactions between two cylindrical conductors. The results are found in the three papers [17]–[19]. The first of the papers deals with the solution for the electrostatic potential in the gap between two slightly shifted cylindrical conductors carrying an arbitrary distribution of voltage and the calculation of the corresponding electrostatic energy as a function of the shift. In the second paper these results are used to derive the expressions of the electrostatic patch forces. The third provides the derivation of the electrostatic torque between two coaxial cylinders and the interesting case of the spin motion is described in detail.

A convenient model of a localized patch suggested in [18] allows us to calculate all the forces and torques in a closed elementary form. In particular, two patches identical up to perhaps the voltage sign, sitting one at each cylinder, produce the following axial force and torque (upper/lower sign goes for patches of the same/opposite sign):

$$F_z/F_* = \pm 4\pi^{3/2}\,\zeta\,\exp\left(-\zeta^2\right)\,\sin^2(\Delta\varphi/2)\,m(\varphi_1-\varphi_2,\Delta\varphi), \quad \zeta=(z_1-z_2)/2\Delta z\,;$$
$$T_z/T_* = \mp\pi^{3/2}\,(\Delta z/4d)\,\exp\left(-\zeta^2\right)\,\sin^6(\Delta\varphi)\,\sin(\varphi_1-\varphi_2)\,\mu(\varphi_1-\varphi_2,\Delta\varphi)\,.$$

Both results hold for coaxial cylinders to lowest order in the cylinder radius to gap ratio, $a/d \ll 1$; $\{\varphi_1, z_1\}$ and $\{\varphi_2, z_2\}$ are the coordinates of the patch centers in cylindrical coordinates, $2\Delta\varphi$ and $2\Delta z$ are the angular and axial widths of the patches, the characteristic values of the force and torque are, respectively, $F_* = \varepsilon_0 V_0^2 a/d$ and $T_* = F_* d = \varepsilon_0 V_0^2 a$, with V_0 being the maximum magnitude of the patch voltage. The coefficients m and μ are bounded periodic functions of the angular patch width ($\lambda \equiv \cos\Delta\varphi$) and their angular separation $\gamma \equiv \varphi_1 - \varphi_2$, namely:

$$m(\gamma,\lambda) = \frac{1-\lambda}{4}\left[1+\frac{(1+\lambda)^2}{2}\,\frac{\cos(\varphi_1-\varphi_2)-\lambda^2}{1-2\lambda^2\cos(\varphi_1-\varphi_2)+\lambda^4}\right];\ \mu(\gamma,\lambda) = \frac{1+\lambda^2}{\left(1-2\lambda^2\cos\gamma+\lambda^4\right)^2}\,.$$

Using these and similar formulas for all the force and torque components up to linear order in the cylinder shift, a detailed analysis of the patch interaction for one pair of patches is carried out, and the dependence of forces and torques on the patch parameters (width and strength) and their mutual position is examined.

PoS(Texas 2010)253

Some estimates and numerical values for PE are provided specifically for the case of the STEP experiment. The formulas for the PE force and torque allow, in fact, for an essentially more realistic modeling of the patch interactions, which can be done in the following way. One represents both patch potentials on the cylindrical surfaces as a superposition of some number of model patches with different voltages, sizes, and positions. By the formulas found in [18, 19], the PE forces and torques caused by these distributions can be explicitly calculated. It leads to the force and torque expression as a quadratic form of the patch voltages with the coefficients depending on all other parameters in a known way.

Having these formulas at hand, one then carries out simulations by specifying parameter sets in various ways and computing the patch forces and torques. One can pick the parameters randomly, and eventually come up with the patch force and torque statistics. One can also use any lab information on the patch distributions, arranging for a semi-random patch sets, as was done, for instance, when simulating magnetic trapped flux distribution on GP-B rotors [20]. Such exhaustive analysis can be strongly recommended before the STEP flight. On the other hand, the same general formulas can be used for fitting control effort data obtained during the experiment, for restoring the voltage patch patterns on the proof masses and bearings. Once the latter are known, the axial forces can be computed, and the systematic experimental error due to them can thus be bounded.

References

[1] Pugh G.E.. *Proposal for a Satellite Test of the Coriolis Prediction of General Relativity.* Memorandum 11, Weapons Systems Evaluation Group, The Pentagon, Washington D. C. (1959), reprinted in 'Nonlinear Gravitodynamics. The Lense-Thirring Effect', ed. by R. J. Ruffini, C. Sigismondi, Word Scientific, Singapore, 2003, p.p. 414.

[2] Lange B.. *The Drag–Free Satellite*. AIAA Journal **2** (9) 1590, (1964).

[3] Bardeen J.. *The Theory of Work Function II. The Surface Double Layer*. Phys. Rev. **49** (9) 653, (1936).

[4] Smoluchowski R. *Anisotropy of the Electronic Work Function of Metals*. Phys. Rev. , **60** 661, (1941).

[5] Darling T.W.. *Electric Fields on Metal Surfaces at Low Temperatures*. Ph.D. Thesis, "School of Physics", University of Melbourne, Parkville, (1989).

[6] Camp J.B., T.W. Darling, and R.E. Brown. *Macroscopic Variations of Surface Potentials of Conductors*. J. Appl. Phys. **69** (10) 7126, (1991).

[7] Rossi F. and G.I. Opat. *Observations of the Effects of Adsorbates on Patch Potentials*. J. Appl. Phys. **25** 1349, (1992).

[8] Speake C.C.. *Forces and Force Gradients due to Patch Fields and Contact–Potential Differences*. Class. Quant. Grav. **13** A291, (1996).

[9] Keiser G.M., J. Kolodziejczak, and A.S. Silbergleit. *Misalignment and Resonance Torques and Their Treatment in the GP-B Data Analysis*. Space Science Reviews **148** (1–4) 383, (2009).

[10] Everitt C.W.F., M. Adams, W. Bencze, et al. *The Gravity Probe B Data Analysis: Status and Potential for Improved Accuracy of Scientific Results*. Space Science Reviews, **148** (1-4) 53, (2009).

[11] Keiser G.M., M. Adams, W.J. Bencze, et al.. *Gravity Probe B*. Rivista del Nuovo Cimento **32** (11) 555, (2009).

PoS(Texas 2010)253

[12] http://einstein.stanford.edu/gallery.

[13] Everitt C.W.F.. *The Stanford Relativity Gyroscope Experiment*. 'Near Zero: New Frontiers of Physics', ed. by J.D. Fairbank, B.S. Jr. Beaver, C.W.F. Everitt, and P.F. Michelson. W.H. Freeman and Co., New York, 1988, p.p.608.

[14] Mester J., et al.. *The STEP Mission: Principles and Baseline Design*. Class. Quant. Grav. **18** 2475, (2001).

[15] Overduin J., C.W.F. Everitt, J. Mester, and P.W. Worden. *The Science Case for STEP*. Adv. in Space Res. **43** 1532, (2009).

[16] Will C. *Progress in Lunar Laser Ranging Tests of Relativistic Gravity*. Phys. Rev. Lett. **93** 261101 (2004).

[17] Ferroni V., A.S. Silbergleit. *Patch Effect in Cylindrical Geometry. I. Potential and Energy between Slightly Non–coaxial Cylinders.*, http://arxiv.org/abs/1009.3292, (2010).

[18] Ferroni V., A.S. Silbergleit. *Patch Effect in Cylindrical Geometry. II. Force.*, http://arxiv.org/abs/1009.3293, (2010).

[19] Ferroni V., A.S. Silbergleit. *Patch Effect in Cylindrical Geometry. III. Torque.*, http://arxiv.org/abs/1009.3294, (2010).

[20] Nemenman I.M., A.S. Silbergleit. *Explicit Green's Function of a Boundary Value Problem for a Sphere and Trapped Flux Analysis in Gravity Probe B Experiment*. J. Appl. Phys., **86** (1) 614, (1999).

PoS(Texas 2010)253